

Stochastic approaches to inflation model building

Erandy Ramírez and Andrew R. Liddle

Astronomy Centre, University of Sussex, Brighton BN1 9QH, United Kingdom

(Dated: September 25, 2018)

While inflation gives an appealing explanation of observed cosmological data, there are a wide range of different inflation models, providing differing predictions for the initial perturbations. Typically models are motivated either by fundamental physics considerations or by simplicity. An alternative is to generate large numbers of models via a random generation process, such as the flow equations approach. The flow equations approach is known to predict a definite structure to the observational predictions. In this paper, we first demonstrate a more efficient implementation of the flow equations exploiting an analytic solution found by Liddle (2003). We then consider alternative stochastic methods of generating large numbers of inflation models, with the aim of testing whether the structures generated by the flow equations are robust. We find that while typically there remains some concentration of points in the observable plane under the different methods, there is significant variation in the predictions amongst the methods considered.

PACS numbers: 98.80.Cq

astro-ph/0502361

I. INTRODUCTION

The impressive results from the Wilkinson Microwave Anisotropy Probe [1] have done much to improve the standing of inflation as the leading paradigm for the origin of structure in the Universe. However, they have not done much in the way of reining in the very large number of viable inflationary models, as the uncertainty in the key prediction of the spectral index n remains significant (and crucially encloses the special value of unity), and there is no sign of primordial gravitational waves (specified by their ratio r relative to density perturbations).

The large collection of inflationary models (see Ref. [2] for extensive reviews) has primarily been developed in an *ad hoc* manner, through selection of potentials motivated either by some considerations from fundamental physics or by simplicity. Typically these potentials may have several parameters, meaning that the best that observations can hope to do is constrain those parameters. Only if the potential is particularly tightly defined, for instance $V(\phi) \propto \phi^6$, can it be ruled out by present observations. Despite the *ad hoc* way in which the collection of models has been constructed, their collective predictions cover a fair part of the n - r observational plane, albeit not evenly. It does not seem appropriate, however, to interpret this as saying that inflation models favour certain types of predictions.

An alternative approach is to throw away the idea of taking input from fundamental physics and of enforcing simplicity (usually on the potential $V(\phi)$ driving inflation), and instead seek to generate models of inflation via some stochastic process, exploiting numerical techniques where appropriate. The archetypal such method is the inflationary flow equations, introduced by Hoffman and Turner [3] and generalized to high order by Kinney [4] (see also Refs. [5, 6, 7]). Intriguingly, models generated via the flow equations exhibit a very clear structure in the observational plane, primarily occupying the line

$r \simeq 0$ or a diagonal locus extending to positive r and negative $n - 1$. The principal aim of this paper is to consider whether or not such a structure is a robust prediction of stochastically-generated inflation models, or whether it is specific to the flow equations implementation. As a by-product, we provide a new implementation of the flow equations, and also explore the origin of their observational prediction more closely. We restrict ourselves to single-field inflation throughout.

II. FLOW EQUATIONS REVISITED

The flow equations take as their starting point a set of differential equations linking a set of slow-roll parameters defined from the Hubble parameter H . Following the notation of Kinney [4], these are

$$\epsilon(\phi) \equiv \frac{m_{\text{Pl}}^2}{4\pi} \left(\frac{H'(\phi)}{H(\phi)} \right)^2; \quad (1)$$

$$\ell \lambda_{\text{H}} \equiv \left(\frac{m_{\text{Pl}}^2}{4\pi} \right)^\ell \frac{(H')^{\ell-1}}{H^\ell} \frac{d^{(\ell+1)}H}{d\phi^{(\ell+1)}}; \quad \ell \geq 1, \quad (2)$$

where primes are derivatives with respect to the scalar field. For example, the parameter ${}^1\lambda_{\text{H}}$ equals $(m_{\text{Pl}}^2/4\pi)H''/H$ and is often denoted $\eta(\phi)$. Using the relation

$$\frac{d}{dN} = \frac{m_{\text{Pl}}^2}{4\pi} \frac{H'}{H} \frac{d}{d\phi}, \quad (3)$$

where we define the number of e -foldings N as decreasing with increasing time, yields the flow equations

$$\begin{aligned} \frac{d\epsilon}{dN} &= \epsilon(\sigma + 2\epsilon); \\ \frac{d\sigma}{dN} &= -5\epsilon\sigma - 12\epsilon^2 + 2({}^2\lambda_{\text{H}}); \\ \frac{d({}^\ell\lambda_{\text{H}})}{dN} &= \left[\frac{\ell-1}{2}\sigma + (\ell-2)\epsilon \right] ({}^\ell\lambda_{\text{H}}) + {}^{\ell+1}\lambda_{\text{H}}; \quad \ell \geq 2, \end{aligned} \quad (4)$$

where $\sigma \equiv 2({}^1\lambda_H) - 4\epsilon$ is a convenient definition.

As pointed out in Ref. [8], these equations actually have limited dynamical input from inflation, since in the form $d/d\phi$ they are a set of identities true for any function $H(\phi)$, and the reparametrization to d/dN modifies only the measure along the trajectories, not the trajectories themselves. In that light it seems surprising that they can say much about inflation at all, but it turns out that the flow equations can be viewed as a (rather complicated) algorithm for generating functions $\epsilon(\phi)$ which have a suitable form to be interpreted as inflationary models [8]. In the following section we will compare their results with more direct ways of generating such functions, but in the meantime we will explore the flow equations themselves further.

A. A new numerical implementation of the flow equations

The standard implementation of the flow equations [4] decides a truncation level for the hierarchy, sets ranges for the slow-roll parameters within which they are randomly selected, and integrates the flow equations either until the end of inflation, $\epsilon = 1$, or until a stable late-time attractor is reached. In the former case the equations are then integrated backwards for a suitable number of e -foldings (either a fixed number such as 50, or one also randomly chosen within a range [4]) where the observational quantities n , r , and possibly others are evaluated and plotted. If a late-time attractor is reached the observables are read off at that point.

Here we use a new and more efficient implementation of the flow equations, exploiting the fact that the flow equations have an analytic solution discovered in Ref. [8]. This is simply a polynomial in $H(\phi)$:

$$H(\phi) = H_0 \left[1 + A_1 \frac{\phi}{m_{\text{Pl}}} + \dots + A_{M+1} \left(\frac{\phi}{m_{\text{Pl}}} \right)^{M+1} \right]. \quad (5)$$

The coefficients A_i can be written in terms of the initial values of the slow-roll parameters as

$$\begin{aligned} A_1 &= -\sqrt{4\pi\epsilon_0}; & A_2 &= \pi(\sigma_0 + 4\epsilon_0); \\ A_3 &= -\frac{4\pi^{3/2}}{3} \frac{{}^2\lambda_{H,0}}{\epsilon_0^{1/2}}; & A_4 &= \frac{2\pi^2}{3} \frac{{}^3\lambda_{H,0}}{\epsilon_0}; \\ A_5 &= -\frac{4\pi^{5/2}}{15} \frac{{}^4\lambda_{H,0}}{\epsilon_0^{3/2}}; & A_6 &= \frac{4\pi^3}{45} \frac{{}^5\lambda_{H,0}}{\epsilon_0^2}; \\ A_7 &= \frac{8\pi^{7/2}}{315} \frac{{}^6\lambda_{H,0}}{\epsilon_0^{5/2}}. \end{aligned} \quad (6)$$

We use the ranges specified in Ref. [4] to randomly choose those values:

$$\begin{aligned} \epsilon_0 &= [0, 0.8]; \\ \sigma_0 &= [-0.5, 0.5]; \end{aligned}$$

$$\begin{aligned} {}^2\lambda_{H,0} &= [-0.05, 0.05]; \\ {}^3\lambda_{H,0} &= [-0.005, 0.005]; \\ &\dots \\ {}^7\lambda_{H,0} &= 0, \end{aligned} \quad (7)$$

where the last closes the hierarchy. To allow direct comparison with Kinney's work, we use these ranges throughout, though one expects the results to be at least modestly dependent on the assumptions made here [4]. However we take the equations to sixth-order, one order higher than Kinney's main results, as one of the methods we will compare with later can only be implemented for even orders. As already shown by Kinney, and separately verified by us, such a change in order has negligible impact on the flow equation predictions. We have carried out flow analyses at fifth and eighth orders as well as those displayed here.

Although this solution is analytic, there is still the need for one integration in order to determine the number of e -foldings as a function of ϕ , from Eq. (3). However this is just a single equation to be integrated, regardless of the order to which the flow equations are taken.

Figure 1 shows the results from the flow equations, with the left-hand panel showing our new implementation based on the analytic solution, and the right-hand panel the traditional multi-equation implementation. The same sequence of 40,000 initial conditions was used in each case, with most of the points finishing at very small r . The values of the spectral index n and tensor-to-scalar ratio r were obtained using second-order expressions and the conventions of Ref. [4]. As expected, the diagrams are essentially identical point-by-point, though some minor differences occur from the way our implementations differ at very small values of ϵ .

The diagram shows a clear and by now well-known structure first noted by Hoffman and Turner [3]; in addition to the majority of the points at small r , there is a swathe of models running in a tightly-defined strip given approximately by $r = 0.3(1-n)$, which is close to but not exactly the same as the power-law inflation condition [4]. While Kinney has been careful not to overinterpret the tendency of points to lie in this vicinity, noting that the measure on initial conditions is unknown, the results are often used to indicate where typical inflationary models might lie (e.g. Ref. [6]). Our main aim in this paper is to investigate the robustness of this structure.

B. Integration direction

First however we investigate in a little more detail how the structure arises. Kinney's main classification of trajectories is into those reaching the late-time attractor (which all have $r \rightarrow 0$ and $n > 1$, corresponding to the field asymptoting into a non-zero minimum of the potential), those trajectories where inflation ends with $\epsilon = 1$, and the rejected set of trajectories which are unable to sustain sufficient inflation. We make a further division of

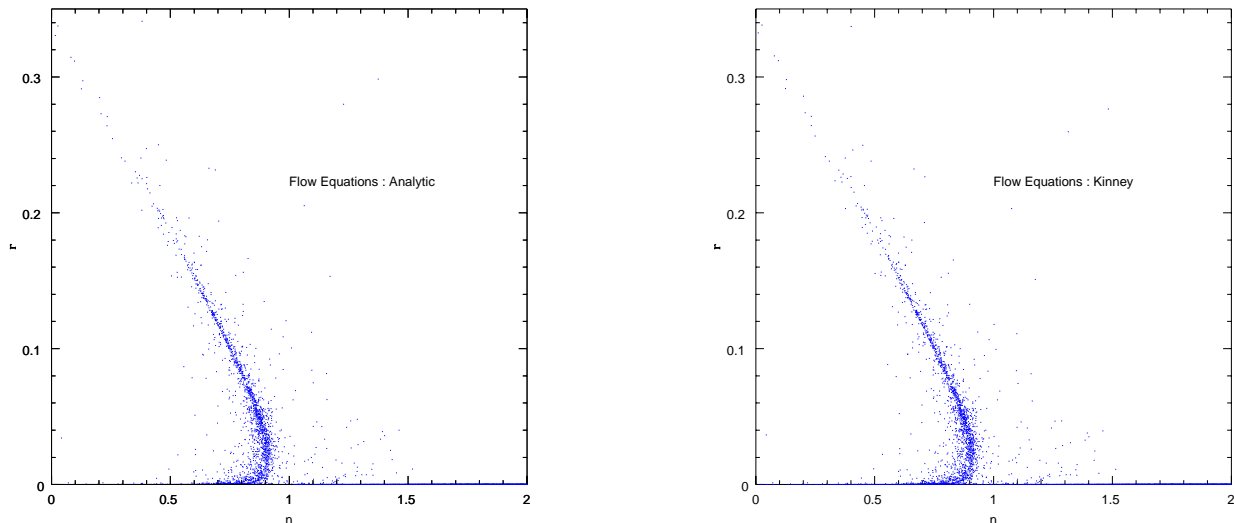


FIG. 1: Observables at second order for 40000 initial conditions. The two figures are essentially identical, and reproduce the results of Fig. 1 in Ref. [4] though at lower point density.

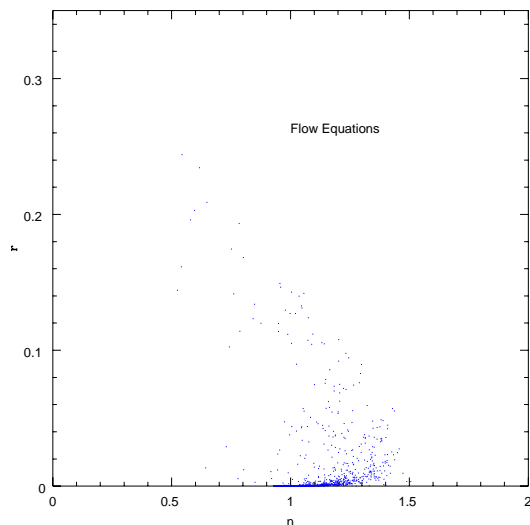


FIG. 2: Points in parameter space finishing inflation with 50 e -foldings or more in the forwards integration.

those trajectories where inflation ends, into those where more than 50 e -foldings of inflation were obtained from the initial point (meaning that the location where the observables were read off was reached by forwards integration from the initial point), and those where less than 50 e -foldings were obtained from the initial point, so that the point corresponding to the observables is effectively obtained by integrating backwards in time from the initial condition.

We find that the vast majority of random initial conditions which end inflation do so before 50 e -foldings are

achieved, in proportion roughly 35 to 1. In Figure 2 we show only points obtained by forwards integration; as there are so few of these we increased the number of initial conditions tested up to 600,000, so as to have a greater density of points (1225 in all, corresponding to just 0.2% of all initial conditions) than in Fig. 1. We find that those points correspond mainly to the region of parameter space where $n > 1$, and do not correspond to the main swathe of points seen in Fig. 1. That swathe is therefore generated entirely from initial conditions that have to be integrated backwards in time. The change of integration direction is significant, because the critical point structure of the system is different in the inverse time direction (the flow will typically be to the peaks of the potential rather than the troughs). Although the backwards integration will pick out those critical points, they need not represent a distribution that might have arisen from whatever mechanism generated the initial conditions.

However even the backwards integration does not explain the flow equations structure, because the only stable critical points under backwards integration are at $r \rightarrow 0$ and $n < 1$. The diagonal swathe is not stable, and, as already shown in Refs. [3, 4], the trajectories evolve along it, typically following quite complicated paths when projected on the n - r plane. Given that the location of the swathe is known, it would be nice to explain that behaviour via an analytic argument, but we have not been able to find an analytic approximation that makes clear why points are able to spend a long time in those parts of the plot.

III. NEW APPROACHES TO STOCHASTIC GENERATION OF INFLATION MODELS

We now turn to alternative methods of generating random inflation models to contrast with the flow equations. As we have seen, the flow equations are equivalent to a Taylor expansion of the function $H(\phi)$, which uniquely specifies the inflationary trajectory. However it is not the only way to do so. Single-field inflation models can also be uniquely specified either by giving the potential $V(\phi)$ or, as noted in Ref. [9], by specifying the function $\epsilon(\phi)$.

In order to investigate the robustness of the flow equation predictions, one should therefore compare its results with those from expansions of these alternative functions, as there is no reason to prefer one over another. We will consider Taylor expansions of both $\epsilon(\phi)$ and $V(\phi)$, and additionally consider a Padé approximant expansion of $\epsilon(\phi)$. In each case we take the randomly-chosen coefficients to correspond to the same ranges of slow-roll parameters used by Kinney for his flow equations analysis [4].

If one of the three functions $H(\phi)$, $V(\phi)$ and $\epsilon(\phi)$ is specified, then the equivalent form of the others can readily be obtained. However once the functions are truncated as expansions at a given order, this correspondence breaks down, e.g. a sixth-order truncation of $H(\phi)$ does not correspond to a sixth-order truncation of $\epsilon(\phi)$. In carrying out these expansions, we are therefore investigating different subsets of the general slow-roll inflation model. Even if the expansions were taken to infinite order the correspondence between models will only be obtained provided each series is within its radius of convergence, which is not guaranteed. On the other hand, by choosing the same initial values for the slow-roll parameters in each case, we are ensuring that the functional forms at the initial point are sampled from the same distribution.

A. $\epsilon(\phi)$ as the fundamental input

The general strategy is similar to the new analytic approach to the flow equations, in that we choose coefficients randomly to generate a function $\epsilon(\phi)$, and then numerically integrate to determine the number of e -foldings supported. However at this point we do have to mention one drawback of using $\epsilon(\phi)$, which is that when the function crosses zero (i.e. into the unphysical region) it typically does so linearly which means it does so in a finite number of e -foldings. By contrast, the $\epsilon(\phi)$ generated from either the Hubble parameter or the potential always approaches zero quadratically, generating an infinite number of e -foldings. The $\epsilon(\phi)$ expansions are therefore unable to generate points corresponding to the late-time attractor.

1. Taylor series expansion

The simplest expansion we can make is a Taylor series

$$\epsilon(\phi) = \sum_{i=0}^K a_i (\phi/m_{\text{Pl}})^i, \quad (8)$$

where we assume $\phi = 0$ initially. The higher slow-roll parameters can all be obtained by differentiating this function, and so we can determine the coefficients by randomly selecting the slow-roll parameters within the same ranges as for the flow equations using those relations. The relations, taking the expansion to sixth-order, are

$$\begin{aligned} a_0 &= \epsilon_0; \\ a_1 &= -\sqrt{4\pi\epsilon_0}(\sigma_0 + 2\epsilon_0), \\ a_2 &= \pi [\sigma_0^2 - 2\epsilon_0\sigma_0 - 12\epsilon_0^2 + 4(^2\lambda_{\text{H},0})]; \\ a_3 &= \frac{4\pi^{3/2}}{3\sqrt{\epsilon_0}} [-3(^2\lambda_{\text{H},0})\sigma_0 + 2\epsilon_0(^2\lambda_{\text{H},0}) + 6\epsilon_0\sigma_0^2 \\ &\quad + 21\sigma_0\epsilon_0^2 + 12\epsilon_0^3 - 2(^3\lambda_{\text{H},0})]; \\ a_4 &= -\frac{\pi^2}{3\epsilon_0} [-12(^2\lambda_{\text{H},0})^2 + 88\epsilon_0\sigma_0(^2\lambda_{\text{H},0}) + 160\epsilon_0^2(^2\lambda_{\text{H},0}) \\ &\quad - 8\sigma_0(^3\lambda_{\text{H},0}) + 4\epsilon_0(^3\lambda_{\text{H},0}) - 45\epsilon_0^2\sigma_0^2 - 312\epsilon_0^3\sigma_0 \\ &\quad - 384\epsilon_0^4 + 6\epsilon_0\sigma_0^3 - 4(^4\lambda_{\text{H},0})]; \\ a_5 &= -\frac{2\pi^{5/2}}{15\epsilon_0^{3/2}} [-240\epsilon_0^4\sigma_0 + 40(^2\lambda_{\text{H},0})(^3\lambda_{\text{H},0}) + 480\epsilon_0^3\sigma_0^3 \\ &\quad + 380(^2\lambda_{\text{H},0})\epsilon_0^2\sigma_0 - 140(^3\lambda_{\text{H},0})\epsilon_0\sigma_0 - 260(^3\lambda_{\text{H},0})\epsilon_0^2 \\ &\quad - 80(^2\lambda_{\text{H},0})\epsilon_0\sigma_0^2 + 1360(^2\lambda_{\text{H},0})\epsilon_0^3 - 200(^2\lambda_{\text{H},0})^2\epsilon_0 \\ &\quad - 1440\epsilon_0^5 + 135\epsilon_0^2\sigma_0^3 + 4(^5\lambda_{\text{H},0}) + 10(^4\lambda_{\text{H},0})\sigma_0 \\ &\quad - 4(^4\lambda_{\text{H},0})\epsilon_0]; \\ a_6 &= \frac{\pi^3}{45\epsilon_0^2} [-840(^2\lambda_{\text{H},0})^2\epsilon_0\sigma_0 + 120(^2\lambda_{\text{H},0})(^4\lambda_{\text{H},0}) \\ &\quad + 5040\epsilon_0^3(^3\lambda_{\text{H},0}) - 768(^4\lambda_{\text{H},0})\epsilon_0^2 - 8(^5\lambda_{\text{H},0})\epsilon_0 \\ &\quad + 1920(^2\lambda_{\text{H},0})^2\epsilon_0^2 - 1920\epsilon_0^4(^2\lambda_{\text{H},0}) - 408(^4\lambda_{\text{H},0})\epsilon_0\sigma_0 \\ &\quad + 10080(^2\lambda_{\text{H},0})\epsilon_0^3\sigma_0 + 1380(^3\lambda_{\text{H},0})\epsilon_0^2\sigma_0 \\ &\quad + 4140(^2\lambda_{\text{H},0})\epsilon_0^2\sigma_0^2 - 300(^3\lambda_{\text{H},0})\epsilon_0\sigma_0^2 + 8(^6\lambda_{\text{H},0}) \\ &\quad + 80(^3\lambda_{\text{H},0})^2 + 135\epsilon_0^2\sigma_0^4 - 2340\epsilon_0^3\sigma_0^3 - 17640\epsilon_0^4\sigma_0^2 \\ &\quad - 1520(^2\lambda_{\text{H},0})(^3\lambda_{\text{H},0})\epsilon_0 + 24(^5\lambda_{\text{H},0})\sigma_0 \\ &\quad - 33120\epsilon_0^5\sigma_0 - 14400\epsilon_0^6]. \end{aligned} \quad (9)$$

We are then able to solve the model using a single integration to find the $N(\phi)$ relation, as in our new flow equations approach. We then apply the same tests to the models thus generated: do they lead to an adequate number of e -foldings, do they require backwards integration to achieve 50 e -foldings, and if satisfactory where do they lie in the observational plane?

2. Padé approximant expansion

A Padé approximant is an alternative to a Taylor expansion, which typically exhibits better convergence properties. It is formed of a ratio of two polynomials, which may have the same or different orders:

$$\epsilon(\phi) = \frac{\sum_{i=0}^M a_i(\phi/m_{\text{Pl}})^i}{1 + \sum_{i=1}^N b_i(\phi/m_{\text{Pl}})^i}. \quad (10)$$

There is a one-to-one correspondence between Padé approximants and Taylor expansions of the appropriate order ($K = M + N$); those expansions then agree near the origin of the expansion but differ as the expansion parameter, in this case ϕ/m_{Pl} , becomes of order one, as is typical in single-field inflation models.

We generate the Padé approximants from the Taylor series using a routine from Numerical Recipes [10]; this routine is restricted to $N = M$ which is why we chose a sixth-order Taylor expansion above. Having generated $\epsilon(\phi)$ in this way, we proceed as before. One additional caveat is that Padé approximants asymptote to constant values; this corresponds to power-law inflation but is somewhat artificial and so we exclude points which require backwards integration to generate 50 e -foldings, and which tend to a constant asymptote between zero and one.

B. $V(\phi)$ as the fundamental input

We can also generate the observables by Taylor expanding the potential and integrating the e -foldings relation to find the values of r and n 50 e -foldings before the end of inflation. A similar expansion was used to investigate inflationary dynamics in Ref. [11], but that paper delineated parameter space regions rather than generating ensembles of models.

We write the potential as

$$V(\phi) = \sum_{i=0}^K v_i(\phi/m_{\text{Pl}})^i. \quad (11)$$

The initial condition ranges that Kinney uses are given in terms of slow-roll parameters defined from the Hubble parameter; to obtain equivalent ranges on the coefficients of the potential we use the first-order slow-roll relations from Ref. [12]. This gives

$$\begin{aligned} v_1 &\simeq -\sqrt{16\pi\epsilon_0}, \\ v_2 &\simeq 4\pi \left(\frac{\sigma_0}{2} + 3\epsilon_0 \right), \\ v_3 &\simeq -\frac{8\pi^2}{3\sqrt{\pi\epsilon_0}} \left[6\epsilon_0^2 + ({}^2\lambda_{\text{H},0}) + \frac{3}{2}\epsilon_0\sigma_0 \right], \\ v_4 &\simeq \pi^2 \left[\sigma_0^2 + 8\epsilon_0\sigma_0 + 16\epsilon_0^2 + \frac{16}{3}({}^2\lambda_{\text{H},0}) + \frac{4}{3}\frac{({}^3\lambda_{\text{H},0})}{\epsilon_0} \right] \end{aligned} \quad (12)$$

$$\begin{aligned} v_5 &\simeq -\frac{8\pi^{5/2}}{3\epsilon_0^{1/2}} \left[\sigma_0({}^2\lambda_{\text{H},0}) + 4\epsilon_0({}^2\lambda_{\text{H},0}) + ({}^3\lambda_{\text{H},0}) \right. \\ &\quad \left. + ({}^4\lambda_{\text{H},0})/(5\epsilon_0) \right] \\ v_6 &\simeq \frac{-2\pi^3}{45\epsilon_0^2} \left[174\epsilon_0^2\sigma_0({}^2\lambda_{\text{H},0}) + 168\epsilon_0^3({}^2\lambda_{\text{H},0}) \right. \\ &\quad \left. + 33\epsilon_0\sigma_0^2({}^2\lambda_{\text{H},0}) + 40\epsilon_0({}^2\lambda_{\text{H},0})^2 + 90\epsilon_0\sigma_0^2({}^3\lambda_{\text{H},0}) \right. \\ &\quad \left. + 360\epsilon_0^2({}^3\lambda_{\text{H},0}) + 72\epsilon_0({}^4\lambda_{\text{H},0}) + 12\sigma_0({}^4\lambda_{\text{H},0}) \right. \\ &\quad \left. + 4({}^5\lambda_{\text{H},0}) \right] \end{aligned}$$

Those relations are also used to evaluate the observables once the position of 50 e -foldings is found.

C. Results

In Figure 3 we plot the results for each expansion for 6000 accepted initial conditions, replotting again the flow equations case with that number of points for comparison. The same range has been chosen for the observables in each case.

Each of the expansions is plotted to sixth-order. In order to check the convergence of the method, we have also analyzed the flow equations at fifth-order (to compare with Kinney [4]) and eighth-order, and the other three methods at fourth-order. With the exception of the Padé approximant for $\epsilon(\phi)$, discussed further below, there were no significant changes in the distributions obtained indicating that reasonable convergence had occurred.

We see that there are significant differences between the models, though each does show some level of concentration in the observable plane. Of the three new methods, the Taylor expansion of the potential gives results closest to the flow equations, showing indications of the same swathe of points with non-zero r , but not however reaching to such high values. The classification of points is very similar to the flow equations, with 90% trivial points, and almost all the remainder requiring backwards integration to achieve 50 e -foldings.

By contrast, the two $\epsilon(\phi)$ expansions give results which are visually quite different. The Taylor series gives a diffuse ensemble of points, with a preference for $n > 1$ but covering a fairly large fraction of the observable plane. The classification of points is also quite different in this case, with a higher fraction of points, about 15%, giving 50 e -foldings of inflation from the forward integration as compared to those requiring backwards integration (recall this method does not generate trivial points).

The Padé approximant expansion of $\epsilon(\phi)$ gives a different outcome again, with the separate classifications of points leading to different groupings in the plane. The vast majority of the points shown correspond to backwards integration. The main feature at $n < 1$ corresponds to $\epsilon(\phi)$ functions which approach zero in the backwards integration, but do generate 50 e -foldings before reaching that point; these generate a similar structure as the flow equations. The grouping of points to the right

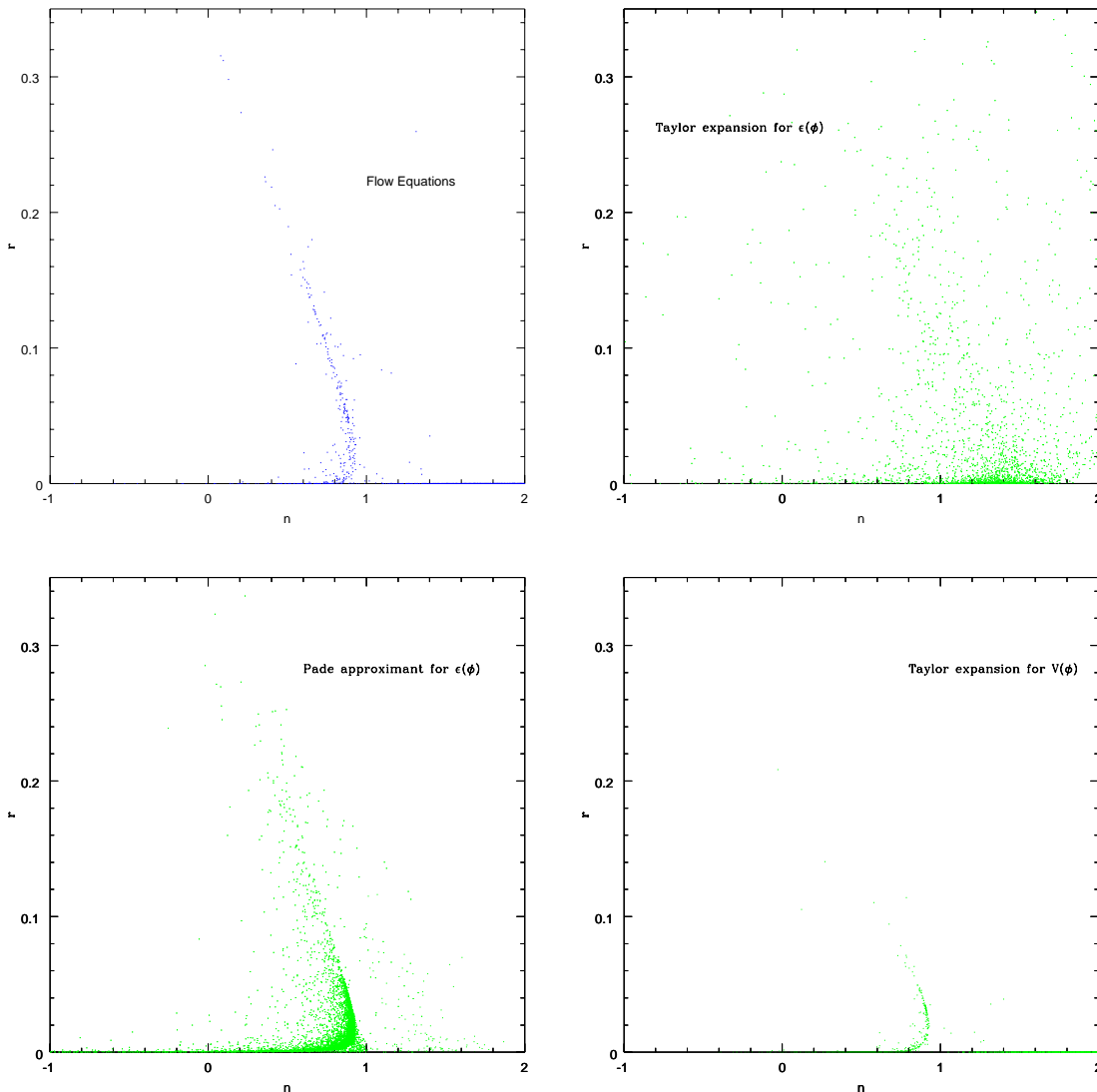


FIG. 3: The distribution in the observable plane for each of the four methods discussed in this paper, in each case for 6000 accepted initial conditions. On the top left are results for the flow equations, to be compared with the Taylor expansion for $\epsilon(\phi)$ (top right), the Padé approximant for $\epsilon(\phi)$ (bottom left) and the Taylor expansion for the potential (bottom right).

of that at high r corresponds to backwards integration points, but this time to functions $\epsilon(\phi)$ which approach one and give 50 e -foldings before that point. There is a third distinct grouping, mainly at $n > 1$ and small r , corresponding to points achieving 50 e -foldings in the forward integration, but it contains very few points (2% of the total).

However it is less easy to draw firm conclusions from the Padé approximant, because we found the method is much less well converged than the others. When we ran this method at fourth-order rather than sixth-order, the same general structures were picked out, but the balance of points was quite different with most of the points lying in the right-hand set rather than the familiar flow equations swathe. By contrast, for the other methods the

results were essentially unchanged between fourth-order and sixth-order.

IV. CONCLUSIONS

We have investigated several ways of randomly generating sets of inflation models, in order to compare their predictions in the observational plane with those of the flow equations approach. We have seen that the different methods, all of which are comparably well motivated, give significantly different predictions.

In two of our new methods, we see hints of the structure seen in the flow equations, but much less well defined. Models lying in that region do seem particularly

well suited to generating a sufficient number of e -foldings, but the narrowness of the band appears to some extent to be an artifact of the flow equations implementation. In particular, a Taylor expansion of $\epsilon(\phi)$, which seems as well motivated as the flow equations approach, does not reproduce such a coherent structure in the observable plane.

Acknowledgments

E.R. was supported by Conacyt and A.R.L. by PPARC. We thank Will Kinney for useful discussions.

E.R. is indebted to Martin Kunz for his valuable help in Fortran and useful discussions and comments. She also thanks Fernando Santoro, Michaël Malquarti, Liam O'Connell, James Fisher, Diana Hanbury, Peter Thomas, David Rowley, Neil Bevis and Jon Urrestilla for their kind help.

-
- [1] C. L. Bennett *et al.*, *Astrophys. J. Supp.* **148**, 1 (2003), [astro-ph/0302207](#); D. N. Spergel *et al.*, *Astrophys. J. Supp.* **148**, 175 (2003), [astro-ph/0302209](#).
 - [2] D. H. Lyth and A. Riotto, *Phys. Rep.* **314**, 1 (1999), [hep-ph/9807278](#); A. R. Liddle and D. H. Lyth, *Cosmological inflation and large-scale structure*, Cambridge University Press, Cambridge (2000).
 - [3] M. B. Hoffman and M. S. Turner, *Phys. Rev. D* **64**, 023506 (2001), [astro-ph/0006321](#).
 - [4] W. H. Kinney, *Phys. Rev. D* **66**, 083508 (2002), [astro-ph/0206032](#).
 - [5] S. H. Hansen and M. Kunz, *Mon. Not. Roy. Astr. Soc.* **336**, 1007 (2002), [hep-ph/0109252](#).
 - [6] H. V. Peiris *et al.*, *Astrophys. J. Supp.* **48**, 213 (2003), [astro-ph/0302225](#).
 - [7] R. Easther and W. H. Kinney, *Phys. Rev. D* **67**, 043511 (2003), [astro-ph/0210345](#); W. H. Kinney, E. W. Kolb, A. Melchiorri, and A. Riotto, *Phys. Rev. D* **69**, 103516 (2004), [hep-ph/0305130](#); C. Chen, B. Feng, X. Wang, and Z. Yang, *Class. Quant. Grav.* **21**, 3223 (2004), [astro-ph/0404419](#).
 - [8] A. R. Liddle, *Phys. Rev. D* **68**, 103504 (2003), [astro-ph/0307286](#).
 - [9] A. R. Liddle, *Phys. Rev. D* **49**, 739 (1994), [astro-ph/9307020](#).
 - [10] W. H. Press, S. A. Teukolsky, W. T. Vetterling, and B. P. Flannery, *Numerical Recipes*, Cambridge University Press (1992).
 - [11] M. Malquarti, S. M. Leach, and A. R. Liddle, *Phys. Rev. D* **69**, 063505 (2004), [astro-ph/0310498](#).
 - [12] A. R. Liddle, P. Parsons, and J. D. Barrow, *Phys. Rev. D* **50**, 7222 (1994), [astro-ph/9408015](#).